Separation Science and Technology
Publication details, including instructions for authors and subscription information:
http://www.informaworld.com/smpp/title~content=t713708471

Biomass-Adsorbent Adhesion Forces as an Useful Indicator of Performance in Expanded Beds

Rami Reddy Vennapusa[a]; Oscar Aguilar[b]; James Maxime Beti Mintong[a]; Gesa Helms[c]; Jürgen Fritz[c]; Marcelo Fernández Lahore[a]
[a] Downstream Bioprocessing Laboratory, School of Engineering and Science, Jacobs University, Bremen, Germany [b] Departamento de Biotecnología e Ingeniería de Alimentos, Centro de Biotecnología, Tecnológico de Monterrey. Campus Monterrey, Monterrey, México [c] Biophysics Laboratory, School of Engineering and Science, Jacobs University, Bremen, Germany

Online publication date: 24 November 2010

To cite this Article Vennapusa, Rami Reddy , Aguilar, Oscar , Mintong, James Maxime Beti , Helms, Gesa , Fritz, Jürgen and Lahore, Marcelo Fernández(2010) 'Biomass-Adsorbent Adhesion Forces as an Useful Indicator of Performance in Expanded Beds', Separation Science and Technology, 45: 15, 2235 — 2244
To link to this Article: DOI: 10.1080/01496395.2010.507664
URL: http://dx.doi.org/10.1080/01496395.2010.507664

Separation Science and Technology, 45: 2235–2244, 2010

ISSN: 0149-6395 print/1520-5754 online
DOI: 10.1080/01496395.2010.507664

Taylor & Francis
Taylor & Francis Group

Biomass-Adsorbent Adhesion Forces as an Useful Indicator of Performance in Expanded Beds

Rami Reddy Vennapusa,[1] Oscar Aguilar,[2] James Maxime Beti Mintong,[1] Gesa Helms,[3] Jürgen Fritz,[3] and Marcelo Fernández Lahore[1]

[1]*Downstream Bioprocessing Laboratory, School of Engineering and Science, Jacobs University, Bremen, Germany*
[2]*Departamento de Biotecnología e Ingeniería de Alimentos, Centro de Biotecnología, Tecnológico de Monterrey. Campus Monterrey, Monterrey, México*
[3]*Biophysics Laboratory, School of Engineering and Science, Jacobs University, Bremen, Germany*

Biomass deposition onto an adsorbent matrix can severely affect early downstream bioprocessing performance e.g., during expanded bed adsorption. Cell deposition phenomena are sensitive to the nature of the interacting cells and matrix bodies and to the solution chemistry, but also depend on the exerted hydrodynamic shear forces. Strong adhesion forces require high hydrodynamic shear for cell detachment, e.g., ≈1400 pN would be needed to detach a yeast cell from a DEAE Sepharose bead. Both adhesion and detachment forces can be reduced by spontaneous coverage of the adsorbent surface with polyvinyl pyrrolidone. For comparison, only ≈270 pN would be required to remove such a cell deposited onto a Chelating-Cu^{2+} bead. First examples of corroborating calculated XDLVO interaction energies by direct force measurements with an atomic force microscopy are presented. Evaluating interfacial forces at the nanoscale can allow for an optimized bioprocess and adsorbent design.

Keywords atomic force microscopy; biomass adhesion; expanded bed; hydrodynamics; integrated downstream bioprocesses

INTRODUCTION

Expanded bed adsorption (EBA) is an advanced unit operation for the purification of biological products in which the clarification, concentration, and purification are integrated in a single step, thus reducing the complexity of primary downstream processing. This, in turn, can reduce the overall biomanufacturing costs. The application of EBA implies, however, that also intact cell particles, cell debris, and suspended materials present in the feedstock will interact—in a minor or larger extent—with fluidized adsorbent beads. The high voidage between the adsorbent beads in the expanded bed allows for the elutriation, but also the deposition, of such particulate entities. The combination of a gentle hydrodynamic environment, a high surface area, and low mixing within the expanded bed makes this system highly susceptible for biocolloid attachment. Unfortunately, unwanted interaction between the biomass and the adsorbent phase may lead to the development of a poor system hydrodynamics and therefore, impaired sorption performance (1,2). Such biomass deposition phenomena have been hampering the industrial utilization of EBA since its introduction in the mid-90s (3). A deeper understanding of the interaction phenomena and forces between chromatographic beads and biomass might therefore help to improve and optimize process performance.

Taking into consideration the complexity of interfacial phenomena at the (sub) micrometer scale, a comprehensive approach should not only consider just purely electrostatic interactions but also other interaction forces especially when applying the principles of colloid chemistry to explain biomass-adsorbent attachment at the local (particle) level (4,5). An extended approach of the Derjaguin-Landau-Verwey-Overbeek (DLVO) theory for biomass adhesion and colloidal stability was already presented elsewhere (6). The XDLVO theory includes a (short-range) acid–base (AB) component besides the long-range interfacial interactions which are electrodynamic "Lifshitz-van der Waals" (LW) and "electrostatic" interactions (EL). The application of these principles to bioprocess science and technology would lead to the development of appropriate tools for better process design and material development for downstream processing. The XDLVO approach has proved successful to explain cell–surface interactions phenomena where hydrophobic (7), hydration (8), and electrostatic (9) forces are dominant. LW and AB forces are experimentally accessible via contact angle measurement with three

Received 28 October 2009; accepted 24 February 2010.
Address correspondence to Marcelo Fernández Lahore, Downstream Bioprocessing Laboratory, School of Engineering and Science, Jacobs University, Campus Ring 1, Bremen 28759, Germany. E-mail: mfernandez-lahore@jacobs-university.de

diagnostic liquids (10). On the other hand, EL forces are accessible by experimental determination of zeta (or streaming) potential values (11).

To understand biomass interaction during direct capture processes, our group has evaluated the total free interfacial energies between different typical chromatography adsorbents and model cells, suspended in an aqueous buffer. Interaction energies were presented as a function of the distance between the mentioned interacting bodies (5,12,13). Such graphs reveal the existence of two regions in the energy landscape of bead-biomass interactions where biomass can be trapped: a primary energy minimum, indicating a strong irreversible interaction, but also a less pronounced secondary energy minimum where particles are more weakly adsorbed, indicating a reversible deposition. These studies are indicating that deposition and re-entrainment of cells can occur within secondary energy minima, at separating distances of a few nanometers. It follows that the "nano-environment" adjacent to the solid surface in buffer media can determine the mechanisms and extent of cell deposition.

The influence of hydrodynamic shear on the attachment and detachment of particles in secondary energy minimum is an important observable fact that has received little attention in the literature (14,15). However, bio-colloidal particles within a secondary minimum are expected to be much more sensitive to hydrodynamic shear than the colloids trapped in a primary minimum because of their weak association with the solid phase (16). Hence, attachment of biocolloids to process surfaces is anticipated to depend on the nature of the interacting surfaces (biomass type/nature of the adsorbent beads), on system hydrodynamics (flow regime), and on solution chemistry (mobile phase composition). The effect of hydrodynamic drag forces on XDLVO primary (irreversible deposition) and secondary minimum (reversible deposition) were experimentally evaluated by Xiaing Li et al. (16). Studies performed observing the deposition of polystyrene colloids on a column packed with glass beads have demonstrated that a hydrodynamic drag force can actually suffice to detach the colloidal particles from the solid surface (17).

Besides being a powerful imaging device, atomic force microscopy (AFM) has evolved as an instrument for measuring actual interaction forces at the nanometer and molecular scale (18–21). AFM allows the assessment of the various types of phenomena occurring during the adhesion or adsorption of biological entities, where a mixture of macro- and microscopic forces are involved. For example, it has been demonstrated that AFM can be applied to measure interaction forces between single cell adhesion molecules but also between microbial cells and a substratum surface, including the contribution of microbial membrane polysaccharides to such interactions (9,22).

The aim of this study was to contribute to the understanding of the interplay between biomass adhesion and hydrodynamic forces in the EBA system. This is a crucial effect related to the overall performance of such primary recovery operations. Moreover, the suitability of AFM to produce independent experimental data on the total interaction force between the biomass and adsorbent beads is highlighted.

MATERIALS AND METHODS

Materials

Chromatographic materials and columns were purchased from GE Healthcare (Munich, Germany). Water was ultrapure quality. All other chemicals are obtained from AppliChem GmbH (Darmstadt, Germany) and were of analytical grade.

Yeast Cells

Yeast cells (*Saccharomyces cerevisiae*) were cultivated, harvested at late exponential phase, and washed three times with dilute buffer solutions (23). Cells were employed for hydrodynamic experiments immediately after harvesting and washing. Intact yeast cell diameter was taken as 8 μm. A Hamaker constant value of 0.34 kT and 0.40 kT for DEAE and Chelating Cu^{+2} beads, respectively, was employed for calculations (24).

Hydrodynamic Experiments

Hydrodynamic experiments were performed in Tricorn™ glass chromatographic columns (5 mm internal diameter, 50 mm length) packed with Streamline™ adsorbents (GE Healthcare, Munich, Germany). These macroporous adsorbents are made of cross-linked agarose (6%) containing a crystalline quartz core. Chelating particles were loaded with copper metal ions utilizing the standard procedures (25). The quality of the packing was evaluated by residence time distribution analysis employing 1% acetone as tracer. Highly porous frits were utilized in order to allow for non-restricted passage of yeast cells through the system (26). The packed material was fully loaded with biological particles by injecting three biomass pulses (4 ml each) at a velocity of $0.9\,m \cdot h^{-1}$. Cell concentration was adjusted to $\approx 6.4 \times 10^7$ cell $\cdot$ cm^{-3} to reach an optical density of 0.8 at 600 nm. Cell number was determined employing a Coulter Counter (Multisizer™ 3, Beckman Coulter, CA, USA). Hydrodynamic experiments were run in an automated ÄKTA Explorer 100 system (GE Healthcare, Munich, Germany). Mobile phase was composed of 20 mM phosphate buffer (pH 7.6) for DEAE beads and 20 mM phosphate buffer (pH 7.6) with 250 mM sodium chloride and 1 mM imidazol for IMAC Cu^{+2} beads. Flow velocities were adjusted according to the system from 1.5 to $90\,m \cdot h^{-1}$. The cumulative peak area as a function of

linear flow velocity ($m \cdot h^{-1}$) was plotted for each system by continuously monitoring the release of particles @ 600 nm. Normalized plots of the cumulative peak area vs. the flow rate were used to estimate the flow velocity at which half of the cumulative peak maxima occurred for both systems. These flow rates were used for the calculation of the hydrodynamic shear rate for each system. Regeneration of the material was performed by extensive treatment with 1 M sodium hydroxide and 1 M imidazol for DEAE beads and IMAC beads, respectively.

Energy Distance Profiles

Free energy of interaction between bodies was calculated as a function of distance as previously described (5), employing the input from experimental contact angles (3 diagnostic liquids) determinations, and zeta potential measurements. XDLVO forces were calculated according to Torkzaban et al. (15).

Atomic Force Microscopy

AFM force measurements with a colloidal probe were carried out using a Multi Mode Picoforce AFM with a Nanoscope IIIa controller (Veeco, Santa Barbara, CA). Colloidal probes were prepared by gluing several ten micrometer Q HyperZ® bead (PALL BioSepra, Cergy, France) at the tip of a triangular silicon nitride cantilever using two-component epoxy glue (Pattex, Düsseldorf, Germany). The cantilever spring constant, which was nominally between $0.005\,Nm^{-1}$ and $0.02\,Nm^{-1}$ (Veeco, Santa Barbara, CA), was determined to be $0.015\,Nm^{-1}$ on average with the thermal tune method. All presented AFM force distance curves were obtained with the same colloidal probe with a bead of around 60 μm, on bare mica and on mica covered with poly-L-lysine in ultrapure water, 1 mM, and 100 mM sodium chloride (NaCl) solutions. For each surface-solution combination, 64 force-distance curves were taken on different places on the sample using a pulling velocity of 2 nm/s. The presented force distance curves are typical examples of these curves.

Sorption Performance

Expanded bed sorption performance was evaluated as previously described (25). Briefly, breakthrough curves were obtained using Streamline materials with an UpFront EBA column (40 cm height and 1 cm inner diameter). The mobile phase was a 20 mM sodium phosphate buffer (pH 7.4; Conductivity 4 mS/cm). Superficial velocity was 152 cm/h. Naked or PVP-covered beads were utilized. For PVP coating, the mobile phase containing 1% PVP 360 (Sigma-Aldrich Chemie GmbH, Steinheim, Germany) was pumped through the column for about ~3 column volumes and then subsequently washed with plain mobile phase for carrying out the sorption experiments. Biomass concentration was 12.0% on wet basis. BSA was employed as a model protein ($C_0 = 4$ mg/ml); protein breakthrough was monitored off-line by the Bradford method with bovine serum albumin as standard. The results are expressed as the ratio between the dynamic binding capacity and the static binding capacity at equilibrium (Q_{dyn}/Q_{eq}).

RESULTS AND DISCUSSION

Biocolloid Deposition on Chromatography Bead Surfaces

During EBA operation, the crude feedstock is normally in contact with the adsorbent beads in the presence of suspended biomass. Cells or cell fragments can attach to the fluidized beads due to adhesion forces of diverse nature. Considering system hydrodynamics, conditions susceptible for the attachment of biomass onto the solid surface will only occur when the resisting torque due to the adhesive (extended) DLVO forces is greater than the applied hydrodynamic torque. In laminar flow systems characterized by a very low Reynolds number, as it is the case for EBA, the lift forces can be considered irrelevant in comparison to drag forces (27). Therefore, when analyzing the biocolloid detachment mechanism the drag force has to be viewed as the main factor inducing biomass particle removal. Alternatively, the hydrodynamic drag force can play a role in preventing biomass deposition (28,29). Figure 1 summarizes the interplay of forces acting on a cell attached to the surface of an adsorbent bead.

Adhesive Forces Acting in EBA

Previous studies, performed with a variety of adsorbent materials, have demonstrated that XDLVO calculations can reasonable predict biomass deposition in EBA systems (5,12,13). Figure 2 shows the correlation observed between

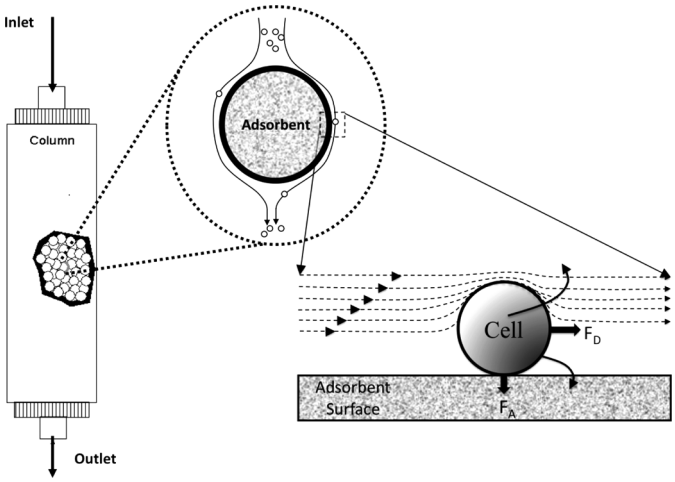

FIG. 1. A simplified schematic representation of the relevant forces during biomass deposition and release from an adsorbent bead. The XDLVO adhesion force (F_A) can be counterbalanced by the hydrodynamic drag force (F_D).

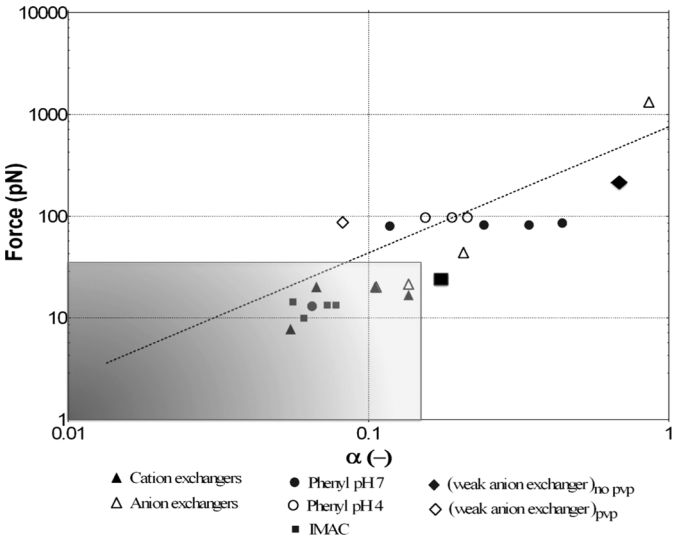

FIG. 2. Correlation between the experimentally observed deposition coefficient (α) and the calculated adhesion force (F_A). Intact yeast cells were employed as biomass type and agarose-based adsorbent beads with various functionalities were used. The points corresponding to the DEAE and Chelating-Cu^{+2} adsorbents are highlighted as large bold symbols. The safe operational region is inside the grey box.

adhesion forces (F_A) for the yeast cell/adsorbent bead pairs and the corresponding (experimental) biomass deposition coefficient (α) values. The parameter α is defined as the probability for a biomass particle to adhere to the surface of the chromatography bead upon collision, under clean bed conditions. This dimensionless parameter takes values from 0 to 1. Values for $\alpha \leq 0.15$ – when determined according to an established routine are generally regarded as appropriate to define safe EBA operation conditions (26). Adhesion forces were estimated according to:

$$F_A = \frac{U_{\min}}{h} \quad (1)$$

Where U_{min} is the absolute value of the secondary (or primary) interaction energy minima, and h is the separation distance between the interacting bodies at which such energy minima occur (15). The free energy of interaction was calculated as per the extended DLVO theory, as previously reported (5) and therefore included Lifshitz-van der Waals, acid-base, and electrostatic double layer interaction energies. XDVLO profiles were calculated using a sphere–plate geometry by assuming that biomass particle diameters are much smaller than bead diameters.

The correlation presented in Fig. 2 indicates that some adsorbent types are prone to biomass fouling, due to an increase in cell deposition and strong adhesion forces between the interacting bodies. Therefore, it was interesting to explore whether an increased adhesion force could be indirectly confirmed by observing the hydrodynamic drag required to remove the deposited cell. In doing so, we chose two different chromatography beads for further study:

a. the anion-exchanger DEAE bead, which would generate a strong adhesion force ($F_A \approx 200$ pN) and,
b. the low-to-moderate interacting copper loaded CHE adsorbent ($F_A \approx 20$ pN).

Systems presenting lower adhesion forces ($F_A < 20$ pN) and, consequently, lower deposition coefficient values ($\alpha \leq 0.15$) should present negligible biomass interactions. Figure 3 depicts the total free energy of interaction (U) vs. distance (H) profiles for the two selected adsorbent beads interacting with a yeast cell, under typical mobile phase conditions. For comparison, the U vs. H curve is shown for a native agarose bead (no ligand, only the bare base matrix). Table 1 shows the calculated total free energy value for the secondary energy minimum, the distance at which this pocket would exist, and more precisely, the corresponding adhesion forces.

Drag Forces Acting in EBA

Biomass particles attach to chromatography beads most likely in the pocket of the secondary energy minimum. It follows that reversible binding shall be observed. Therefore, it is reasonable to assume that hydrodynamic shear caused by the incoming mobile phase (or feedstock) would produce cell detachment if sufficiently high drag forces are exerted on the attached cells or biomass. The hydrodynamic drag force can be determined according to Li et al. (16):

$$F_D = (1.7)6\pi\,\mu\,\nu\,a_c \quad (2)$$

where a_c is the radius of the retained biomass particle, μ is the fluid viscosity, ν is the fluid linear flow velocity, and

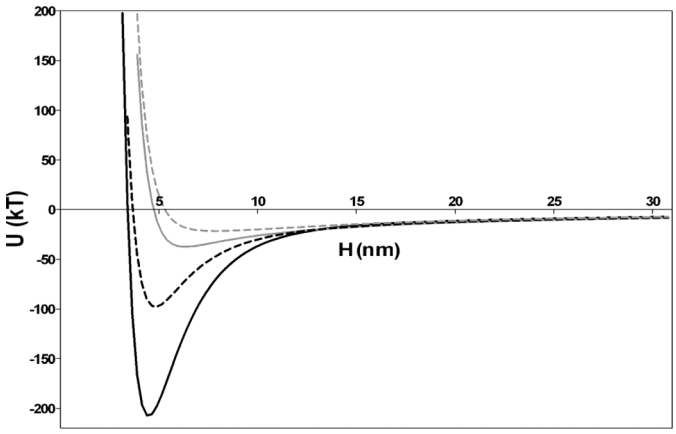

FIG. 3. Total free energy of interaction (U) as function of distance (H) between intact yeast cells and several adsorbent types. Shown are the secondary energy minima. Mobile phase compositions are assumed to be the ones commonly employed for each chromatography mode. DEAE (—); $[DEAE]_{pvp}$(– –); CHE Cu^{+2} (—); Agarose bead (– –).

TABLE 1
Calculated free energy of interaction, adhesion force and hydrodynamic shear force for the systems under study. Errors from input values are below 5%

Condition	Free energy (kT)	Distance (nm)	Adhesion force (pN)	Hydrodynamic shear force (pN)
DEAE/Yeast	−207	4.4	194	1430
$(DEAE)_{pvp}$/Yeast^{+}	−98	4.9	82	ND*
CHE Cu^{+2}/Yeast	−37	6.4	24	277
Agarose Bead	−21	7.9	12	ND*

*ND: Not determined.
$(DEAE)_{pvp}$: DEAE bead coated with 1% w/v PVP 360.
+The XDLVO parameters used to compute U (h) curve for $[DEAE]_{pvp}$ are Hamaker constant 0.37 kT, acid-base free energy $+20\,mJ/m^2$, zeta potential for $(DEAE)_{pvp}$ coated is +5 mV where as for yeast is −18 mV. For the others pairs the XDLVO parameters are published elsewhere (24).

the leading coefficient of 1.7 accounts for wall effects near the adsorbent surface.

In this study, chromatography beads were loaded with yeast cells under standard operational conditions and subsequently, the amount of detached cells was observed as a function of a stepwise increase of the superficial velocity (shear stress) under which the collector system was operated (Fig. 4). The two selected interacting pairs, namely DEAE/yeast cell and CHE/yeast cell, exhibited very different detachment behavior. The observed effect was quantified by defining a threshold superficial velocity required to elute 50% of the bound cells ($F_{H50\%}$). The $F_{H50\%}$ for two pairs were obtained by fitting the experimental data in the sigmoidal dose response model. This parameter can be expected to be a function of biomass type and cell wall composition, solution chemistry and ionic strength, and contact time (30). All these factors have already been taken into account for biomass deposition and sorption performance in expanded bed systems (25,31).

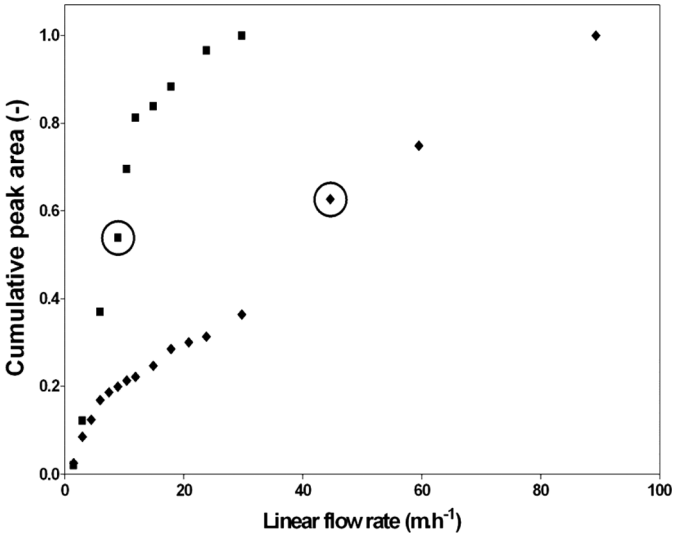

FIG. 4. Hydrodynamic biocolloid removal experiments. A strong interacting adsorbent DEAE (◆) and a low-to-moderate interacting adsorbent CHE-Cu^{+2} (■) were utilized with yeast cells as a model biomass type. Once cells were deposited on the collector surface, cell release from the adsorbent was studied as a function of the linear flow rate. For DEAE two different populations (early and late release) could be identified. The $F_{H50\%}$ was obtained by fitting the experimental data in the sigmoidal dose response model. $F_{H50\%}$ are circled in the figure which are utilized for the calculation of hydrodynamic drag force.

As said, Fig. 4 depicts the effect of an increasing hydrodynamic force on microbial cell detachment from the chromatography beads. For the low-to-moderate CHE/yeast cell pair, a rapid and complete removal of the attached cells can be observed: increasing the flow rate from $1\,ml \cdot min^{-1}$ ($3.0\,m \cdot h^{-1}$) to $5\,ml \cdot min^{-1}$ ($15\,m \cdot h^{-1}$) caused the release of ≥90% of the deposited biomass. The superficial velocity required to elute 50% of the bound cells ($F_{H50\%}$) was $\approx 3\,ml \cdot min^{-1}$ ($9.0\,m \cdot h^{-1}$). A mono-modal distribution of exiting cell particles can be observed. On the contrary, for the strongly interacting DEAE/yeast cell pair, a bi-modal distribution was observed within the microbial cell population leaving the collector surface: a first sub-population of cells are behaving similarly to the CHE/yeast cell system (e.g., $F_{H50\%} = 6\,m \cdot h^{-1}$ i.e., $2\,ml \cdot min^{-1}$) while a second sub-population has required a much higher flow velocity to actually be removed by the hydrodynamic drag applied (e.g., $F_{H50\%} = 45\,m \cdot h^{-1}$ i.e., $15\,ml \cdot min^{-1}$). This observation can be explained by considering the existence of dual deposition which may be driven by heterogeneity in surface characteristics among the microbial cell population. Charge heterogeneity, which is relevant to deposition on anion exchangers, is known to exist in several types of biomass particles (32,33). Therefore, different orientation of the attached cell on the bead surface may cause a differential release of them. Since the bi-modal distribution was observed in the DEAE/yeast but not in the CHE/yeast system, heterogeneity on the porous media is less likely to be the reason for the segregation of two existing sub-populations. Other factors to

be considered in explaining the above-mentioned results are hydrodynamic collisions between mobile and attached cells that result in the escape of weakly bound biocolloids (34), the deformability of microbial cells (35), the presence of microscale flow fluctuations at the collector surface, and cell detachment and subsequent re-entrainment at lower flow velocities (32). Since approximately 70% of the initially loaded yeast cells were detached within the second sub-population, at higher superficial velocities, we adopted the corresponding $F_{H50\%}$ parameter as the characteristic value for the calculation of the hydrodynamic drag force. Table 1 shows the calculated values for the hydrodynamic drag forces for the DEAE/cell and the CHE/cell systems. It can be observed that the force required for cell detachment is roughly 10 times higher than the corresponding adhesion force. These values would overestimate the hydrodynamic force necessary to prevent adhesion.

Counteracting Adhesive Forces: Bead Shielding

The reduction of the adhesive force between a chromatography bead and biomass-biocolloids in the feedstock would facilitate the removal of such particles and therefore would promote biomass elutriation from the EBA system, with very positive consequences on process performance.

Several studies have demonstrated that a "conditioning film" can form on the surface of collector (adsorbent) beads which thereby either increase or decrease biomass deposition on the naked surfaces. Whether a facilitated cell deposition or a protective effect against biomass is produced depends on the physicochemical nature of the film. In a bioprocess context such a film could be produced, e.g., by macromolecules that are present in the fermentation broth. The formation of the conditioning film would then be related to the spent culture media but would also be a function of the processing (contact) time during EBA. An increased biomass deposition with EBA processing time has been already reported (25,1). A conditioning film caused by the culture media could also be the reason why simple measurements performed on cell or cell debris particles and adsorbent beads alone may fail to predict actual process performance. Moreover, such a film could also explain why different feedstock histories may produce changes in overall bed hydrodynamics and sorption performance. Summarizing, there is a need to study each combination of biomass/soluble component(s)/adsorbent bead to fully understand deposition behavior; this has to include the possible change in surface properties with time.

Besides the negative consequences that a macromolecular film with sticky characteristics may have, an opportunity window opens for those chemical additives that possess the following properties:

a. They strongly adhere spontaneously to the chromatography bead by self-assembling,
b. they counteract cell deposition by interfering with otherwise existing biomass to surface interactions,
c. they do not interfere with product binding, and
d. they are safe for using in bioprocessing.

In a previous study, we have observed that polyvinylpyrrolidone (PVP 360), a synthetic polymer of pharmaceutical grade, can actually offer such advantages. On one hand, PVP 360 can form hydrogen bonds with the hydroxyl groups present on the agarose backbone of a bead which leads to cooperative multipoint attachment and film formation (36,37). Due to the high molecular weight of the polymer only superficial attachment is possible, therefore avoiding ligand masking which remain available for bioproduct binding and capture. XDLVO calculations performed assuming a coated-bead vs. a native counterpart showed an important reduction in the total interaction energies (Fig. 3). Calculated interaction energies with yeast cells in 20 mM phosphate buffer showed a ≈ -200 kT minima occurring at a 4.4 nm distance for naked bead but a much lower ≈ -100 kT minima for the PVP-conditioned bead at 4.9 nm distance (Table 1). Consequently, also a decrease in the adhesion force with the PVP-coated DEAE bead can be observed (Table 1). Furthermore, these calculations correlated with cell deposition experiments and cell partition tests (5).

The formation of a cell-repelling conditioning film would have a positive impact on the hydrodynamic condition of the expanded bed and, consequently, would produce an increased sorption performance than the one expected with a naked adsorbent. To link process performance with the events predicted at the micro- nano- scales, dynamic sorption performance was evaluated *via* breakthrough curve analysis. Table 2 shows the observed

TABLE 2
Dynamic binding capacity (Q_{dyn}) as compared to the equilibrium binding capacity (Q_{eq}) obtained during EBA. BSA was utilized as model protein in 20 mM sodium phosphate buffer (pH 7.4). DEAE-Streamline adsorbents were employed. Yeast cells were used as model biomass at a 12% concentration (wet basis). Standard deviations from the experimental values are below 5%

BSA on streamline DEAE[§]		Q_{eq} ($kg\,m^{-3}$)	Q_{dyn} ($kg\,m^{-3}$)	Q_{dyn}/Q_{eq}
Cell free solution	Naked	74.0	51.1	0.69
	PVP-coated*	72.0	48.2	0.67
Biomass	Naked	60.0	20.6	0.34
	PVP coated*	71.1	43.4	0.61

[§]12 cm settled bed height; 1.0 cm inner column diameter; $C_o = 4\,mg \cdot ml^{-1}$; $U = 150\,cm \cdot hr^{-1}$.

*1% w/v polyvinylpirrolidone 360.

dynamic binding capacity (Q_{dyn}) as compared to the equilibrium binding capacity (Q_{eq}) for DEAE-Streamline. To simulate a real process, the expanded bed was loaded with an artificial feedstock composed of BSA (4 mg/ml) and intact yeast cells (12.0%; wet basis); the feedstock was applied at a superficial velocity equal to 150 cm/h. In these experiments a correlation could be established between the sorption ability of the system in buffer where proper fluidization is assumed or verified with conservative tracers- and its resulting sorption performance in the presence of biomass, typically in the range 2% to 12% (wet basis). It was observed (see Table 2) that the ratio Q_{dyn}/Q_{eq} decreased in the presence of cells from ≈0.69 (buffer) to ≈0.34 (biomass) when naked DEAE beads were employed. On the contrary, when using PVP-conditioned beads the mentioned performance indicator was marginally reduced from 0.67 (buffer) to 0.61 (biomass). For comparison, the low-to-moderate interaction CHE/yeast pair rendered under very similar conditions a ratio of 0.82 (buffer) and 0.79 (biomass) (25). Therefore, the formation of a shielding film could open the way for a more efficient protein capture in those systems which are more sensitive to the presence of biomass.

The preceding information is also useful to analyse which consequences can be expected when the shear rate is modified: A naked DEAE-bead interacting with a yeast cell would present an adhesion force of ≈200 pN while the conditioned (or shielded) DEAE-bead would allow for a reduction of this force to ≈80 pN. The shielded system would then show adhesion forces and would be sensitive to hydrodynamic shear, which are much closer to the CHE/yeast pair, a less problematic combination (12). In this case, a reduced adhesion force goes in line with an easier detachment e.g., when the exerted hydrodynamic shear force is close to ≈270 pN.

As a conclusion to this section it can be stated that:

a. The formation of a shielding film results in lower biomass adhesion forces to anion-exchanger materials,
b. with a shielding film attached biomass can be removed easily by the flowing mobile phase or other mechanical means (e.g., movable parts) and,
c. sorption performance can be improved by polymer shielding.

In Table 1 it was observed that the hydrodynamic shear force required to remove an attached cell has to be 10 times higher than the corresponding adhesion force; both forces can be decreased by shielding.

Probing Adhesion Forces: The Role of AFM

Using Atomic Force Microscopy (AFM) to understand the properties of bioprocess materials e.g., nano- and ultra-filtration membranes, as well as their interactions with bioparticles and macromolecules is well established. AFM measurements could help to prove, by an independent experimental method, the appropriateness of XDLVO calculations to predict biomass deposition in EBA. So far XDLVO-like interactions between commercial adsorbent beads and typical biomass components in EBA have not been verified by distance-dependent measurements of the involved interactions. They rely so far on single parameter measurements (such as contact angle and zeta potential) from which distance dependent interaction energies have been calculated.

In a preliminary attempt to evaluate the suitability of AFM measurements to understand the interaction of adsorbent beads with model surfaces, we chose a standard adsorbent bead, a Q Ceramic HyperZ® bead (positively charged) which was attached to an AFM cantilever (Fig. 5). Instead of using a whole yeast cell as a complex test system we chose two simple and well-defined model surfaces to test our approach to correlate surface thermodynamics data with AFM measurements. With the modified cantilever we then probed two model surfaces: hydrophilic mica (negatively charged) and poly-L-lysine modified mica (positively charged). These systems were chosen to simulate charge effects which can occur under real process conditions (5).

Figures 6 a,b show the experimental AFM forces—distance curves between a Q-HyperZ® bead to mica and to poly-L-lysine as a function of sodium chloride concentration. Both sets of curves are taken during the approach of the bead towards the surface. Figure 6a shows the so called "snap-in": the bead gets attracted to the surface when the force gradient of the interaction exceeds the cantilever spring constant and jumps to the surface. The snap-in force decreases with increasing salt concentration and is basically no longer present at 100 mM salt.

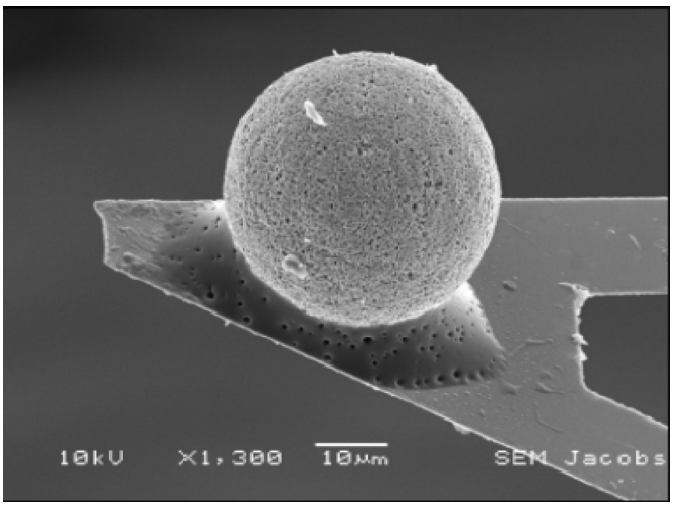

FIG. 5. A 60 µm QHyperZ bead attached to a triangular silicon nitride AFM cantilever.

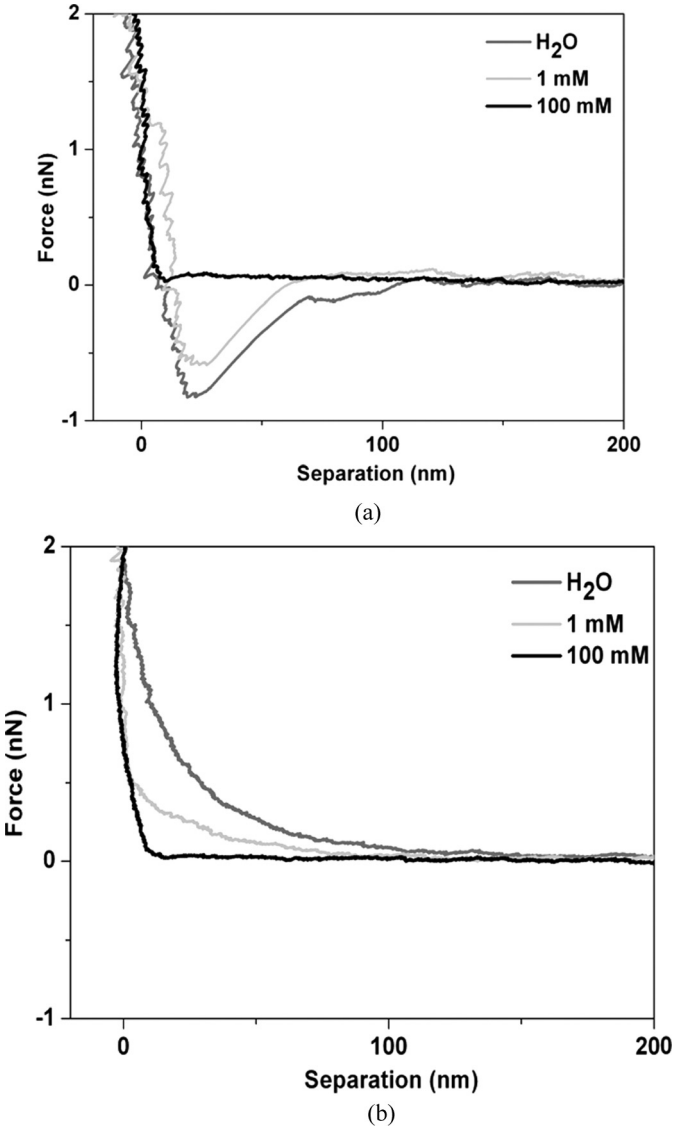

FIG. 6. Representative AFM force curves. An AFM cantilever with a QHyperZ bead attached to it is approached towards a plane mica surface and a mica surface covered with PLL at different sodium chloride concentrations. (a) Shows the attraction between the positive bead and negative surface during approach of the cantilever. (b) Shows the electrostatic repulsion between the positively charged surfaces and positive bead.

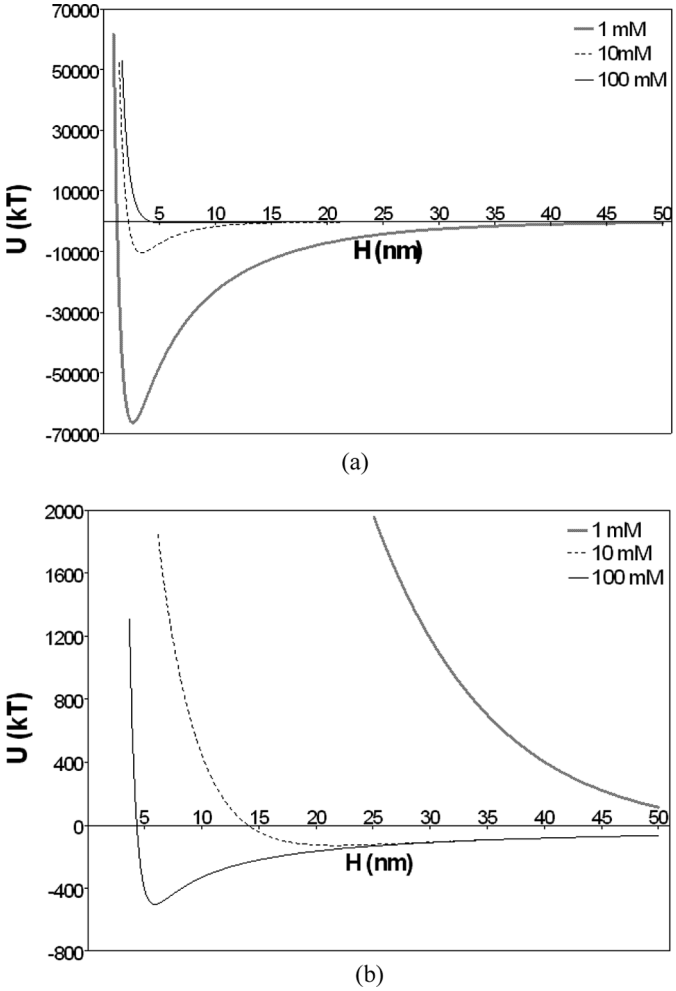

FIG. 7. Total free energy of interaction as function of distance calculated for the same materials and geometry as in the AFM experiment (Fig. 7): (a) Q-hyper Z and mica (b) QHyperZ and PLL surface at different sodium chloride concentrations.

Figure 6b demonstrates the electrostatic repulsion between the two positive surfaces and the increasing shielding of the forces with increasing salt concentration.

So far, the AFM measurements were in qualitative agreement with calculated XDLVO profiles for the same interacting bodies (Fig. 7a/b). Corresponding XDLVO profiles were calculated from the experimentally determined surface energy and streaming or zeta potential parameters reported in literature (38–41). Future experiments will investigate the interaction of different chromatographic beads with different molecules and up to entire cells immobilized on an opposing surface and relevant for EBA. As demonstrated, AFM can measure the presence of long range forces between the beads and the sample, but also (not shown here) the adhesion forces between two interaction surfaces after initial contact. The measurement of adhesion forces is also influenced by contact time and maximum forces applied during contact, both of which might influence or favor e.g., conformational changes between interacting surface-biomass systems. In addition, other time-dependent phenomena such as the swelling of chromatographic beads upon change in salt concentration, or the fouling of one of the surfaces after many approach-retract cycles have to be taken into account when analyzing AFM force curves. Summarizing, AFM measurements could provide in the near future a complementary approach for the direct measurement of adhesion forces in the context of EBA, especially when extended from

molecular model systems to well-defined cell components and entire cells. These measurements, in turn, would allow for better operational control, process design, and the improvement of existing adsorbents.

CONCLUSIONS

Adhesion forces between biomass and chromatography beads can be calculated from interfacial free energies of interaction. Such adhesion forces are useful parameters that allow a better understanding and prediction of EBA performance. A strong interaction force would result in increased biomass deposition and, consequently, impaired sorption performance. These interaction forces are related to the chromatography mode (nature of the adsorbent), to the feedstock characteristics (type of biomass, soluble components), and to the solution chemistry (process mobile phase). Additionally, understanding adhesion forces permit an evaluation of the potential effect of hydrodynamic drag forces that are exerted on the already deposited biomass. The hydrodynamic regime could be tailored to counteract adhesion; this could explain the efficiency of flow distribution systems which have introduced movable parts or denser adsorbents that require increased fluidization velocities. In this study, the force required for cell detachment was found to be roughly 10 times higher than the corresponding adhesion force. It has also been shown that, in some cases, the adhesion force can be modified by simple polymer coating.

Further, the XDLVO interfacial energies for two model interacting surfaces were compared with direct force measurements using atomic force microscopy. A good qualitative agreement was observed. These observations confirm the appropriateness of our approach and open the way for direct measurement of adhesion forces at the nanoscale.

ACKNOWLEDGEMENTS

RRVP gratefully acknowledges a postdoctoral fellowship from the European Commission (5130-50276). We thank Richa Sharma and Veit Wagner for the electron microscopy imaging work.

REFERENCES

1. Fernandez-Lahore, H.M.; Kleef, R.; Kula, M.; Thommes, J. (1999) The influence of complex biological feedstock on the fluidization and bed stability in expanded bed adsorption. *Biotechnol. Bioeng.*, 64 (4): 484.
2. Lin, D.Q.; Fernández-Lahore, H.M.; Kula, M.R.; Thömmes, J. (2001) Minimising biomass/adsorbent interactions in expanded bed adsorption processes: A methodological design approach. *Bioseparation.*, 10 (1–3): 7.
3. Curbelo, D.R.; Garke, G.; Guilarte, R.C.; Anspach, F.B.; Deckwer, W.D. (2003) Cost comparison of protein capture from cultivation broths by expanded and packed bed adsorption. *Eng. Life Sci.*, 3 (10): 406.
4. Van Oss, C.J. (2006) *Interfacial Forces in Aqueous Media*, 2nd Ed.; Taylor & Francis: New York.
5. Vennapusa, R.R.; Hunegnaw, S.M.; Cabrera, R.B.; Fernandez-Lahore, M. (2008) Assessing adsorbent-biomass interactions during expanded bed adsorption onto ion exchangers utilizing surface energetics. *J. Chromatogr. A.*, 1181 (1–2): 9.
6. Bos, R.; Van der Mei, H.C.; Busscher, H.J. (1999) Physico-chemistry of initial microbial adhesive interactions–its mechanisms and methods for study. *FEMS Microbiol. Rev.*, 23 (2): 179.
7. Van Oss, C.J. (1995) Hydrophobicity of biosurfaces – Origin, quantitative determination and interaction energies. *Colloids Surf. B: Biointerfaces*, 5 (3–4): 91.
8. Strevett, K.A.; Chen, G. (2003) Microbial surface thermodynamics and applications. *Res. Microbiol.*, 154 (5): 329.
9. Camesano, T.A.; Logan, B.E. (2000) Probing bacterial electrosteric interactions using atomic force microscopy. *Environ. Sci. Technol.*, 34 (16): 3354.
10. Sharma, P.K.; Rao, K.H. (2002) Analysis of different approaches for evaluation of surface energy of microbial cells by contact angle goniometry. *Adv. Colloid Interface. Sci.*, 98 (3): 341.
11. Lin, D.Q.; Zhong, L.N.; Yao, S.J. (2006) Zeta potential as a diagnostic tool to evaluate the biomass electrostatic adhesion during ion-exchange expanded bed application. *Biotechnol. Bioeng.*, 95 (1): 185.
12. Vennapusa, R.R.; Aasim, M.; Cabrera, R.; Fernandez-Lahore, M. (2009) Surface energetics to assess biomass attachment onto immobilized metal-ion chromatography adsorbents in expanded beds. *Biotechnol. Bioprocess Eng.*, 14 (4): 419.
13. Vennapusa, R.R.; Tari, C.; Cabrera, R.; Fernandez-Lahore, M. (2009) Surface energetics to assess biomass attachment onto hydrophobic interaction adsorbents in expanded beds. *Biochem. Eng. J.*, 43 (1): 16.
14. Shiragami, N.; Hakoda, M.; Enomoto, A.; Hoshino, T. (1997) Hydrodynamic effect on cell attachment to microcarriers at initial stage of microcarrier culture. *Bioprocess Biosyst. Eng.*, 16 (6): 399.
15. Torkzaban, S.; Bradford, S.A.; Walker, S.L. (2007) Resolving the coupled effects of hydrodynamics and DLVO forces on colloid attachment in porous media. *Langmuir.*, 23 (19): 9652.
16. Li, X.; Zhang, P.; Lin, C.L.; Johnson, W.P. (2005) Role of hydrodynamic drag on microsphere deposition and re-entrainment in porous media under unfavorable conditions. *Environ. Sci. Technol.*, 39 (11): 4012.
17. Bergendahl, J.; Grasso, D. (2000) Prediction of colloid detachment in a model porous media: Hydrodynamics. *Chem. Eng. Sci.*, 55 (9): 1523.
18. Kienberger, F.; Kada, G.; Mueller, H.; Hinterdorfer, P. (2005) Single molecule studies of antibody-antigen interaction strength versus intra-molecular antigen stability. *J. Mol. Biol.*, 347 (3): 597.
19. Rief, M.; Oesterhelt, F.; Heymann, B.; Gaub, H.E. (1997) Single molecule force spectroscopy on polysaccharides by atomic force microscopy. *Science*, 275 (5304): 1295.
20. Vadillo-Rodriguez, V.; Busscher, H.J.; Norde, W.; de Vries, J.; Dijkstra, R.J.B.; Stokroos, I.; Van der Mei, H.C. (2004) Comparison of atomic force microscopy interaction forces between bacteria and silicon nitride substrata for three commonly used immobilization methods. *Appl. Environ. Microbiol.*, 70 (9): 5441.
21. Willemsen, O.H.; Snel, M.M.E.; Cambi, A.; Greve, J.; De Grooth, B.G.; Figdor, C.G. (2000) Biomolecular interactions measured by atomic force microscopy. *Biophys. J.*, 79 (6): 3267.
22. Razatos, A.; Ong, Y.-L.; Sharma, M.; Georgiou, G. (1998) Molecular determinants of bacterial adhesion monitored by atomic force microscopy. *Proc. Natl. Acad. Sci. U.S.A.*, 95 (19): 11059.
23. Ganeva, V.; Galutzov, B.; Teissie, J. (2004) Flow process for electroextraction of intracellular enzymes from the fission yeast, *Schizosaccharomyces pombe*. *Biotechnol. Lett.*, 26 (11): 933.
24. Vennapusa, R.R.; Binner, S.; Cabrera, R.; Fernandez-Lahore, M. (2008) Surface energetics to assess microbial adhesion onto fluidized chromatography adsorbents. *Eng. Life Sci.*, 8 (5): 530.

25. Fernandez-Lahore, H.M.; Geilenkirchen, S.; Boldt, K.; Nagel, A.; Kula, M.R.; Thommes, J. (2000) The influence of cell adsorbent interactions on protein adsorption in expanded beds. *J. Chromatogr. A.*, 873 (2): 195.
26. Tari, C.; Vennapusa, R.R.; Cabrera, R.B.; Fernandez-Lahore, M. (2008) Colloid deposition experiments as a diagnostic tool for biomass attachment onto bioproduct adsorbent surfaces. *J. Chem. Technol. Biotechnol.*, 83: 183.
27. Freitas, A.M.; Sharma, M.M. (1999) Effect of surface hydrophobicity on the hydrodynamic detachment of particles from surfaces. *Langmuir.*, 15 (7): 2466.
28. Boks, N.P.; Norde, W.; van der Mei, H.C.; Busscher, H.J. (2008) Forces involved in bacterial adhesion to hydrophilic and hydrophobic surfaces. *Microbiology*, 154 (10): 3122.
29. Johnson, W.P.; Li, X.; Assemi, S. (2007) Deposition and re-entrainment dynamics of microbes and non-biological colloids during non-perturbed transport in porous media in the presence of an energy barrier to deposition. *Advances in Water Resources.*, 30 (6–7): 1432.
30. Mercier-Bonin, M.; Ouazzani, K.; Schmitz, P.; Lorthois, S. (2004) Study of bioadhesion on a flat plate with a yeast/glass model system. *J. Colloid Interface. Sci.*, 271 (2): 342.
31. Vergnault, H.; Willemota, R.-M.; Bonin, M.M. (2007) Non-electrostatic interactions between cultured *Saccharomyces cerevisiae* yeast cells and adsorbent beads in expanded bed adsorption: Influence of cell wall properties. *Process Biochem.*, 42 (2): 244.
32. Simoni, S.F.; Harms, H.; Bosma, T.N.P.; Zehnder, A.J.B. (1998) Population heterogeneity affects transport of bacteria through sand columns at low flow rates. *Environ. Sci. Technol.*, 32 (14): 2100.
33. Ujam, L.B.; Clemmit, R.H.; Chase, H.A. (2000) Cell separation by expanded bed adsorption: use of ion exchange chromatography for the separation of *E. coli* and *S. cerevisiae*. *Bioprocess Eng.*, 23 (3): 245.
34. Bolster, C.H.; Mills, A.L.; Hornberger, G.M.; Herman, J.S. (2001) Effect of surface coatings, grain size, and ionic strength on the maximum attainable coverage of bacteria on sand surfaces. *J. Contam. Hydrol.*, 50 (3–4): 287.
35. Boonaert, C.J.P.; Toniazzo, V.; Mustin, C.; Dufrêne, Y.F.; Rouxhet, P.G. (2002) Deformation of l*actococcus lactis* surface in atomic force microscopy study. *Colloids Surf. B Biointerfaces*, 23 (2–3): 201.
36. Napper, D.H. (1983) *Polymeric Stabilization of Colloidal Dispersions*; Academic Press: New York.
37. Pattanaik, M.; Bhaumik, S.K. (2000) Adsorption behaviour of polyvinyl pyrrolidone on oxide surfaces. *Mater. Lett.*, 44 (6): 352.
38. Brant, J.A.; Johnson, K.M.; Childress, A.E. (2006) Examining the electrochemical properties of a nanofiltration membrane with atomic force microscopy. *J. Memb. Sci.*, 276 (1–2): 286.
39. Harnett, E.M.; Alderman, J.; Wood, T. (2007) The surface energy of various biomaterials coated with adhesion molecules used in cell culture. *Colloids Surf. B Biointerfaces*, 55 (1): 90.
40. Maruyama, A.; Ishihara, T.; Kim, J.-S.; Kim, S.W.; Akaike, T. (1997) Nanoparticle DNA carrier with poly(**L**-lysine) grafted polysaccharide copolymer and poly(**D,L**-lactic acid). *Bioconjug. Chem.*, 8 (5): 735.
41. Vergnault, H.; Mercier-Bonin, M.; Willemot, R.M. (2004) Physico-chemical parameters involved in the interaction of *Saccharomyces cerevisiae* cells with ion-exchange adsorbents in expanded bed chromatography. *Biotechnol. Prog.*, 20 (5): 1534.